

BRAIN TUMOR DETECTION USING DISCRETE WAVELET TRANSFORM AND HYBRID PSO-ACO OPTIMIZED FEED FORWARD NEURAL NETWORK

V. Kavitha ^{*1} and K. Ulagapriya ²

¹Research Scholar, Computer Science and Engineering, Vels Institute of Science Technology, and Advanced Studies

²Associate Professor, Computer Science and Engineering, Vels Institute of Science Technology, and Advanced Studies

*Corresponding Author
V. Kavitha

Article History

Received: 17.09.2025
Revised: 08.10.2025
Accepted: 29.10.2025
Published: 29.11.2025

Abstract:

The development of computer aided diagnosis has been rapid. Its accuracy in detecting abnormalities in brain scans is very important for treating patients. There are various machine learning tools that are designed to analyze the data presented by MRI images. Existing methods are prone to errors, limited learning process, and efficiency issues. In this work, a novel method is presented that addresses these issues by incorporating the Weiner filter. It is also equipped with various other features such as 2D-DWT, PPCA, and LDA. The proposed method is based on the use of a feed-forward neural network and a modified particle swarm optimization technique. It is able to improve the accuracy and stability of its analysis while overcoming the fitting issues encountered in brain scans.

Keywords:

Discrete Wavelet Transformation, Ant Colony Optimization, Feed forward Neural Network (FNN), Weiner Filter, Modified Particle Swarm Optimization, Probabilistic principle component analysis, Linear Discriminant Analysis.

INTRODUCTION

One of the most common and deadly diseases that affects people is brain tumours. The PBDS is a system that can detect the presence of brain tumors. It is capable of making the right diagnosis and treatment decisions [1]. The PBDS utilizes MRI, which is an advanced imaging technique that's used to examine the brain. Compared to other methods, such as X-Ray and CT-Scan, MRI produces clear images of brain tissues. Its properties make it an ideal tool for diagnosing brain disorders. Unfortunately, it can be very time consuming and challenging to analyze the vast amount of brain images that are generated by MRI. With the help of an automated system, it can now perform the procedure in a more accurate and faster manner [2-3].

Despite the numerous algorithms that have been proposed for the PBDS, it is still in its early stages due to the complexity of the process of feature extraction and the classification of images. This paper aims to improve the PBDS' accuracy. Section 2 also covers the latest developments in the field of brain image classification. Section 3 presents the methodology for developing the proposed model for the PBDS system. Section 4 explores the experimental evaluation of the suggested framework with varying parameters. The Section 5 wraps up the work on the research.

1. Related Work

In the past few years, [4] various researchers have proposed methods for the classification of brain images. One of these is the use of a 2D-DWT sub-band approximation for extraction of features. The authors [5] used the DAUB-4 filters for their decomposition algorithm. The two classifiers, which achieved a 98% accuracy, are the SVM and the self-organization mappings. The authors [6] of this study proposed a better DWT for the extraction of features from brain MRI images. They used the feed forward and k-nearest neighbor approach to differentiate normal and abnormal images. Their algorithm's accuracy was almost 97% and 98%, respectively. The authors [7] of this study used a hybrid approach to extract features from brain images. They used various image classifiers, such as the feed forward ANN [7], adaptive chaotic PSO [8], kernel SVM [9-10], and KSVM+PSO [11], for their classification. They also developed a Ripplet transformation that can extract different features from MRI images. The LS-SVM and PCA techniques [12] were utilized for the reduction of the feature and for identifying the non-diseased and diseased brains in MRI scans. The proposed method exhibited high classification accuracy when applied to large sets of data. The proposed method [13] utilized the DAUB-4 wavelet's entropy and the PNN algorithm for processing brain images. The researchers noted that their algorithm's success rate was higher than that of other algorithms [46-50].

MATERIAL AND METHODS:

Nomenclature

Symbol	Explanation
K	N×N MR images
FM	Feature Matrix
M	Number of Features
wac()	Wavelet approximation coefficients
E _M	Empty matrix
E _v	Empty vector
I	Magnetic Resonance Image
O,P	Empty vectors
PPCA()	Probabilistic principle component analysis function
η	Normalized FM
μ	Mean
S	Standard deviation
ρ	Reduced FM
S _w	Singular Scalar Matrix

1.1 Wiener Filter

The Wiener filter is used for preprocessing the MR images. This method is used to decrease the signal noise by replacing the impulse filter [14]. The inverse filtering is to recover the image when it is blurred due to the low pass filter. But, the additive noise effects the inverse filtering. Wiener Filtering is one of the approaches which provide trade-off between the noise smoothing and inverse filtering that provides the noise smoothing and inverts the image blurring. Wiener Filtering uses the stochastic framework for applying the linear approximation to the original Brain MR image. Eq. 1 shows the Wiener filtering method in preprocessing stage at Fourier domain.

$$W_F(f_1, f_2) = \frac{S_x(f_1, f_2)B^*(f_1, f_2)}{S_n(f_1, f_2) + \|B(f_1, f_2)\|^2 S_x} \quad \text{-----}(1)$$

Where $B(f_1, f_2)$ represents the blurring filter, $S_x(f_1, f_2)$ represents the original Brain MR image power spectrum, $S_n(f_1, f_2)$ represents the adaptive noise.

1.2 Feature Extraction

The Discrete wavelet transform (DWT) is the efficient approach used by the wavelet transform (WT). The WT uses the dyadic scales as well as positions [15]. The basic of DWT is described as follows: Consider that $x(t)$ be the square integral function. $\Psi(t)$ is the real valued wavelet related to the $x(t)$ given as

$$W_\psi(\alpha, \beta) = \int_{-\infty}^{\infty} x(t) \frac{1}{\sqrt{\alpha}} \psi\left(\frac{t - \beta}{\alpha}\right) dt \quad \text{-----}(2)$$

Where $W_\psi(\alpha, \beta)$ represents the wavelet transform, α and β represents the dilation factor and translation parameter. Eq. 3 shows the discrete variation of Eq. 2 which can be obtained by restraining α and β to a discrete lattice ($\alpha=2^j$ and $\beta=2^j k$).

$$DWT_{f(n)} = \begin{cases} a_{j,k}(n) = \sum_n x(n) G_j^*(n - 2^j k) \\ d_{j,k}(n) = \sum_n x(n) H_j^*(n - 2^j k) \end{cases} \quad \text{-----}(3)$$

Where $a_{j,k}(n)$ denotes approximation coefficients and $d_{j,k}(n)$ represents the detailed components. $G(n)$ denotes the low pass filter and $H(n)$ denotes the high pass filter respectively. The wavelet scale factors is represented with j and wavelet translation factors is represented with k . Fig. 3 shows the representation of the 2D-DWT where it is applied in each dimension to the image. Here, a sample pathological brain image is taken and applied the three level decomposition of WT.

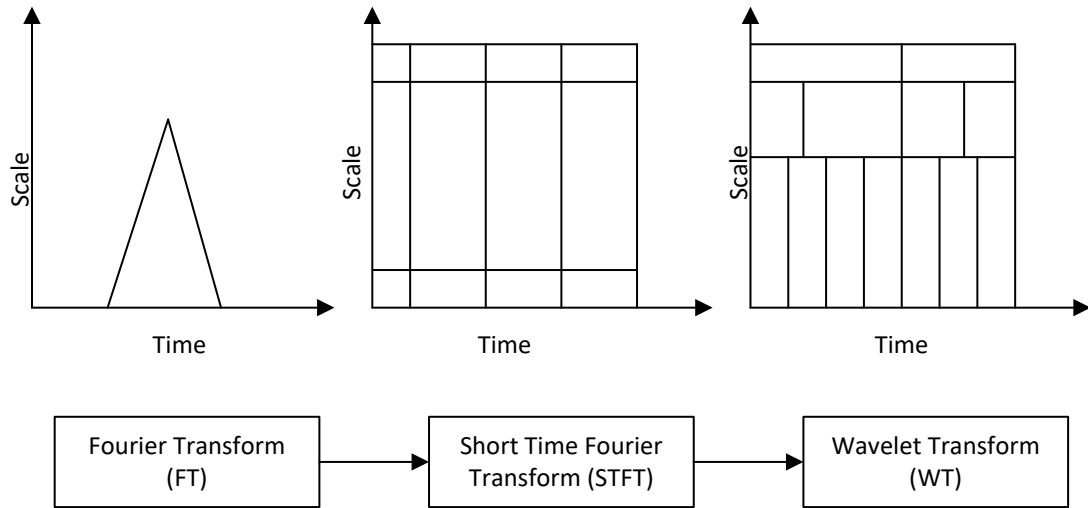


Figure 2: Signal Progression Analysis [15]

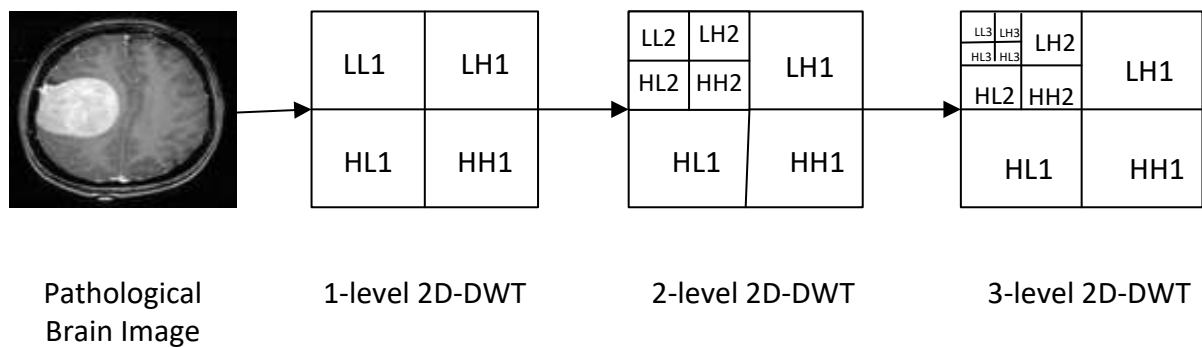


Figure 3: Three-Level 2D-DWT Decomposition on Pathological Brain Image [15]

Figure 3 shows the four sub bands of the image such as LL1, LH1, HL1 and HH1 at level 1. The sub band LL1(a_j) is again decomposed by using 2D-DWT and can be considered for approximating the components. The LH1(d_j^h), HL1 (d_j^v) and HH1 (d_j^d) sub bands are considered for detailed component analysis in horizontal direction, vertical direction and diagonal direction. There are different types of wavelet transforms gain popularity in the wavelet analysis. Haar Wavelet is one among them which is used regularly in different applications [16]. Haar Wavelet shows good performance in noise conditions and also it is having orthogonal as well as symmetric in nature. The Haar wavelet extract the basic components present in the image with high performance. In the proposed work, the approximation coefficients are computed in the level-3 Haar wavelet decomposition image and those are used as the image feature vectors. Algorithm 1 shows the feature extraction procedure for brain MR images.

Algorithm 1: Feature Extraction for Brian MR images

Input: K

Output: FM [L, M], M, wac(), E_M , E_V , I_j

Begin

1. Set $i=1$, $M \rightarrow N/8 \times N/8$
2. Initialize $E_M[1:N/8, 1:N/8]$, $E_V[1, 1:M]$
3. For j in 1 to K do
4. $E_M[1:N/8, 1:N/8] \rightarrow wac(I_j)$
5. While $i \leq M$ do
6. For α in 1 to (N/8) do
7. For β in 1 to (N/8) do
8. $E_V[1, 1:M] \rightarrow E_M[\alpha, \beta]$
9. $i++$
10. End for
11. End for
12. End While
13. Obtain FM which contain all vectors E_V

14. End for

End

1.3 Feature Normalization and Reduction

It is observed that the features computed from the Algorithm 1 has high dimensionality and also requires huge space and computation power. Therefore, there is a requirement of feature reduction techniques to reduce the dimensionality and extract the candidate features. Probabilistic principle component analysis (PPCA) [17] is one of the important approach which reduces the high dimension features in to low dimension features by connecting them to u which is a P-dimensional observation vector and v which is a k-dimensional unobserved vector that is performing normalization with zero mean and unit variance. Algorithm 2 shows the normalization with PPCA.

Algorithm 2: Feature Normalization and Reduction

Input: FM [L, M], M, O[1, 1:M], P[1, 1:M], PPCA()

Output: η [1: L, 1: M], $\mu()$, $S()$, ρ [1: L, 1 : R]

Begin

1. Initialize η , O, P
2. O[1, 1:M] $\rightarrow \mu(\text{FM})$
3. P[1, 1:M] $\rightarrow S(\text{FM})$
4. for i in 1 to m do
5. η [1: L, 1: M] $\rightarrow (\text{FM}[1: L, i] - \text{O}[1, i]) / \text{P}[1, i]$
6. End for
7. Select R
8. Initialize ρ [1: L, 1 : R]
9. ρ [1: L, 1 : R] $\rightarrow \text{PPCA}(\eta, R)$
10. Retrieve ρ

End

From algorithm 1, it is observed that a normalized FM of size $L \times M$ is obtained after applying the PPCA and reduced FM of size $L \times R$ is obtained. The size of the reduced FM is less than the normalized FM. The PPCA removes the class labels for the data and the data will be in the unsupervised mode. To overcome this, Linear Discriminant Analysis (LDA) is introduced. LDA is a supervised approach which distinguishes the classes which is far from the similarities in the data. Conventional LDA is not suitable for the small sample dataset problems and high dimensional features. In this scenarios, LDA forms only singular scalar matrix (S_w) [18]. To overcome this issue, PPCA+LDA is used in the proposed model, where P dimensional data is reduced using the PPCA and K dimensional data is reduced using LDA [19].

1.4 Classification using the FNN and MPSOACO

The combination of feed forward neural network (FNN) and Modified Particle Swarm Optimization with Ant Colony Optimization is used to improve the accuracy, stability and minimizing the overfitting issues in the classification of brain MR images.

1.4.1 Feed Forward Neural Network (FNN)

FNN is the well-known pattern recognition classifier and widely used by many researchers from past decade. The training data set is given as input to the FNN and it performs the batch mode training [20]. The configuration of network is given as $H_{ip} \times H_{hl} \times H_{op}$, here, the two layer neural network with input layer H_{ip} , Hidden layer H_{hl} and output layer H_{op} identifying that the brain is normal or pathological.

Consider that ω_1 and ω_2 is the weighted matrix between the H_{ip} and H_{hl} respectively. Then the following steps are used to update the weighted values to train the data set [21].

Step1: The H_{hl} outputs are estimated using the Eq. 4

$$A_j = f_{hl} \left(\sum_{i=1}^{H_{ip}} \omega_1(i, j) c_i \right) \text{ where } j = 1, 2, \dots, H_{hl} \quad \text{-----}(4)$$

Here c_i represents the i^{th} input value in the network, A_j represents the hidden layer output, f_{hl} represents the H_{hl} activation function and the sigmoid function is shown in Eq. 5.

$$f_{hl}(c) = \frac{1}{1 + \exp(-c)} \quad \text{-----}(5)$$

Step 2: The H_{op} outputs are estimated using the Eq. 5

$$B_j = f_{op} \left(\sum_{i=1}^{H_{hl}} \omega_2(i, k) A_i \right) \text{ where } k = 1, 2, \dots, H_{op} \quad \text{-----}(6)$$

Where f_{op} denotes the H_{op} activation function and the values to the weights are assigned randomly.

Step 3: The MSE is used to expressed the error based on the difference between the target value and output value [22-24].

$$E_l = MSE \left(\sum_{k=1}^{H_{op}} (B_k - T_k) \right) \text{ where } l=1,2,...H_s \quad \text{-----}(7)$$

Where T_k denotes the authentic variables k^{th} value which is available with the user. H_s denotes the number of samples.

Step 4: The fitness function for the H_s samples are given as

$$F(\omega) = \sum_{i=1}^{H_s} E_l \quad \text{-----}(8)$$

Where ω denotes the vectors of (ω_1, ω_2) .

1.4.2 Modified Particle Swarm Optimization (MPSO)

The PSO is the one of the efficient optimization algorithms introduced by [25-26]. The PSO mechanism is used for searching process through the group of particle which will be updated iterative procedure. To find the optimal solution, every particle moved in the direction local best (P_{best}) or global best (g_{best}) in the group [24].

$$P_{best}(i, v) = \arg \min_{k=1...v} [f(P_i(k))], i \in \{1, 2, ..., T_p\} \quad \text{-----}(9) \quad g_{best}(v) = \arg \min_{i=1...T_p, k=1...v} [f(P_i(k))] \quad \text{-----}$$

----- (10)

Where, T_p represents the total particles present in the swarm, v denotes the current iteration value, i denote the index of the particle, f represents the function and P denotes the particle position. Eq. 11 is used to update the position P and velocity V of the particles.

$$V_i(v+1) = V(v) + a_1 r_1 (P_{best}(i, v) - P_i(v)) + a_2 r_2 (g_{best}(v) - P_i(v)) \quad \text{-----}(11)$$

$$P_i(v+1) = P_i(v) + V_i(v+1) \quad \text{-----}(12)$$

Where a_1 and a_2 are the accelerated coefficients, r_1 and r_2 is the random variables which is lies in between 0 and 1.

In [27], the authors proposed modified PSO (MPSO) by adding the inertia ω in to the Eq. 11

$$V_i(v+1) = \omega * V(v) + a_1 r_1 (P_{best}(i, v) - P_i(v)) + a_2 r_2 (g_{best}(v) - P_i(v)) \quad \text{-----}(13)$$

Where inertia ω represents the weight factor which balances the local search and global search.

1.4.3 Ant Colony Optimization mechanism (ACO)

ACO algorithm was proposed in [27] has been proven effective in solving many optimization issues [28-30]. In the ACO algorithm, ants simultaneously search paths to the food. The ants choose the paths based on the pheromone left by the ants in the different paths. The probability of selecting the path is depended on the quantity of the pheromone collected in the particular path. Eq. 14 shows the probability computation for selecting the path.

$$\tau_{ij} = \frac{\chi_{ij}}{\sum_j \chi_{ij}} \quad \text{-----}(14)$$

Where χ_{ij} represents the pheromone intensity of the i^{th} ant in the j^{th} path way. K is used to identify whether the j^{th} path need to be selected or not. T_{ij} is the probability of selecting the i^{th} ant based on the j^{th} path intensity. The fitness function for the feature subset generated at the time of ant reaches food is evaluated using the Eq. 15.

$$fit = \frac{AC}{1 + \lambda n} \quad \text{-----}(15)$$

Where AC denotes the feature subset accuracy, n denotes the number of ants in the feature subset, λ denotes the weight factor. After finishing one cycle, the pheromone values of all paths are updated. Eq. 16 shows the pheromone update mechanism.

$$\chi_{ij}(t+1) = (1 - \rho)\chi_{ij}(t) + \Delta\chi_{ij} \quad \text{------(16)}$$

Where $\Delta\chi_{ij}$ is the incremental value of the pheromone update and ρ denotes the expiration of pheromone update trail. $\Delta\chi_{ij}$ is further explained as follows.

$$\Delta\chi_{ij} = \begin{cases} fit^b, & Path \in S \\ 0, & otherwise \end{cases} \quad \text{------(17)}$$

In Eq. 17, S denotes the set of paths and b denotes the control parameter used for regulating the pheromone quantity.

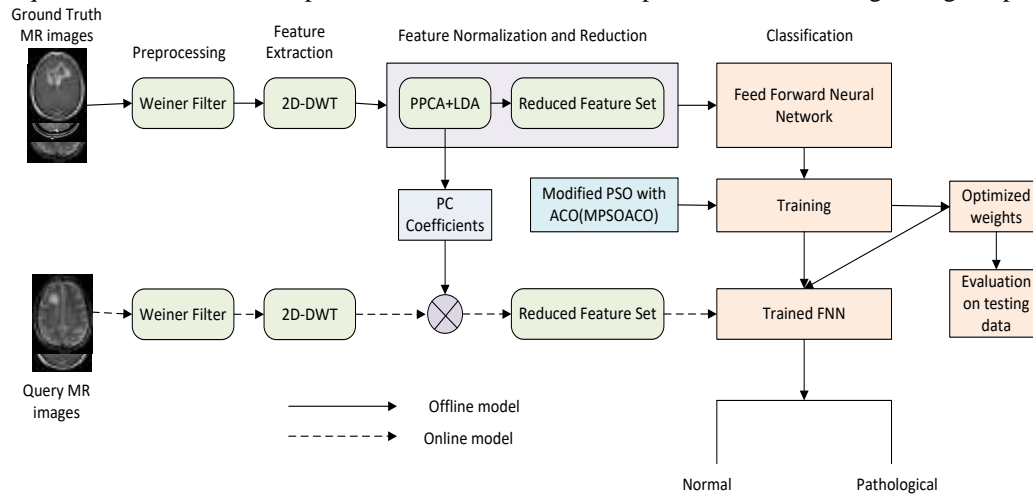


Figure 4: Block diagram of the proposed PBD system

1.4.4 Propose method

The proposed method is composed of four modules: Preprocessing, feature extraction, feature normalization and reduction, and classification. Figure 4 shows the flow chart of the proposed PBD model. The preprocessing is done by using the wiener filter, the feature extraction is carried out using the 2D-DWT, Feature normalization and reduction is processed by PPCA and LDA and the classification is performed using the FNN and MPSOACO. Algorithm 3 shows the detailed analysis of the proposed pathological brain detection system.

Algorithm 3: Proposed PBD model

Input: N-> Number of Brain MR images,
Output: Classified images (Normal or pathological)

Begin

Offline learning:

1. for i in 1 to N do
2. Apply wiener filter for all the images to improve the contrast
3. Apply three level 2D-DWT and create a set of feature vectors with dimension P
4. end for
5. for j in 1 to N do
6. Execute PPCA and LDA transmission for obtaining wavelet coefficients
7. end for

8. perform the cross validation on the generated data set and generate the training data, validation data and testing data
9. Train the FNN algorithm using the MPSOACO algorithm and select the optimal weights at input layer and hidden layer.
10. Calculate the output layer weights using the optimal weights at input layer and hidden layer.
11. Measure the performance of the classifier based on the testing data set.

Online learning:

1. User submit the query image to the system
2. Apply wiener filter for the image to perform preprocessing
3. Apply three level 2D-DWT and create a set of feature vectors with dimension P
4. Obtain reduced feature set by multiplying the wavelet coefficient with feature vector coefficients.
5. Input the reduced feature set to the FNN classifier which is trained by MPSOACO and find the image is normal or pathological

End

2. Experimental analysis

The proposed model simulated using the MATLAB 9.5 R2018b in a PC having the configuration of 3.7 GHz, 12 GB RAM with windows 10 operating system. The performance evaluation of the proposed model is compared with the other existing systems.

Table 1: Parameter setting for K-fold validation for datasets

Datasets	Total Samples		Training		Testing		Validation	
	Usual	Unusual	Usual	Unusual	Usual	Unusual	Usual	Unusual
D-255	35	220	21	132	7	44	7	44
D-160	20	140	12	84	4	28	4	28
D-66	18	48	12	32	3	8	3	8

2.1 Dataset and Cross validation

To measure the performance of the proposed model, three data sets such as D-66 [32], D-160 [33] and D-255 [34] that are having the 66, 160 and 255 images which is of 256×256 in plane resolution [31]. Figure 5 shows the k-fold cross validation of data sets. The pathological brain image data set contains the different type of diseases such as Cerebral toxoplasmosis, Sarcoma, Herpes Encephalitis, Creutzfeldt-Jakob Glioma, Meningioma, Huntington's disease, Alzheimer's disease, Cerebral calcinosis, motor neuron and pick's disease figure 6 shows the sample ground truth brain MR Images. Table 1 shows the different phases of validation. For each disease, we randomly selected 20 images. Hence, there is one usual brain and 7 unusual brains. In the dataset 66, 18 normal brains and 48 pathological brains are selected. In dataset 160, 20 normal brains and 140 pathological brains are selected and in dataset 255, 35 normal brains and 230 pathological brains are selected.

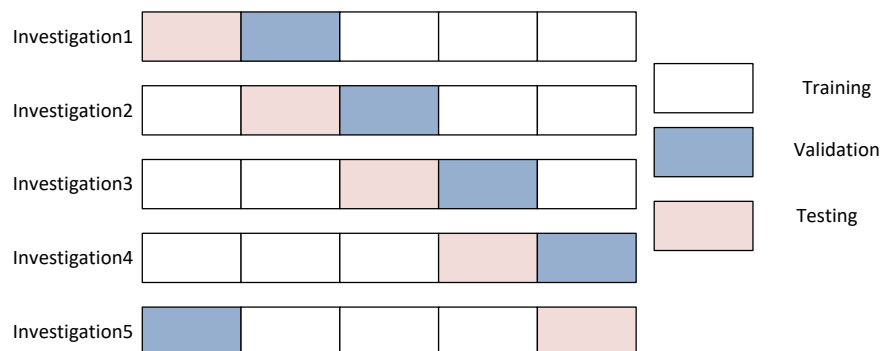


Figure 5: k-fold Cross Validation for Single Iteration

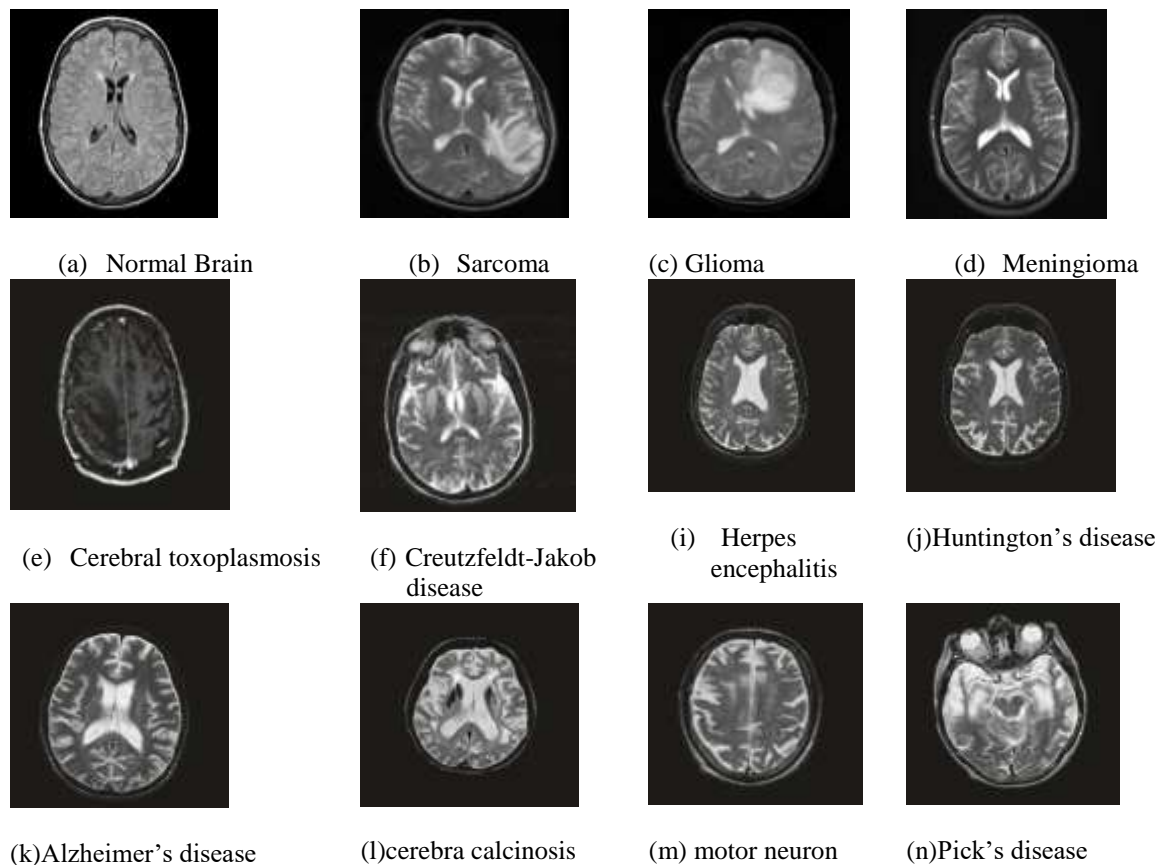


Figure 6: Sample Ground Truth Brain MR Images

4.2 Feature Illustration and Reduction results

First we performed, Wiener filter to improve the contrast of the images. Then, we carried three level 2D-DWT method (Algorithm 1) to divide the image into 10 sub-bands as shown in figure 3. This produces $32 \times 32 = 1024$ feature coefficients. The top left corner in the three level 2D-DWT image denotes the approximation coefficients. The size of the images is taken as $256 \times 256 = 65536$ which is of larger size.

We applied PPCA+LDA on the D-66, D-160 and D-255. Each image in the datasets is rearranged with a row vector and all the images are arranged in the form of two dimensional matrix. Algorithm 2 shows the normalization mechanism using the PPCA+LDA. It reduces the features from 65536 to 1024 by considering the three level 2D-DWT transformations. Figure 7 shows the cumulative variance based on the principle components (features). It is identified that PCA requires 13 features whereas PCA+LDA and PPCA+LDA require only 3 features when the threshold is fixed as 0.95. Therefore, PPCA+LDA is selected as suitable mechanism for identifying the significant components.

4.3 Performance evaluation of FNN-MPSOACO

To classify the Brain MR images into usual or unusual images, we developed the neural network mechanism called as FNN-MPSOACO classifier. The performance of the proposed FNN-MPSOACO classifier is tested with different number of features along with the accuracies of D-66, D-160 and D-255. Table 2 shows the classification accuracy of the proposed method with existing KNN, BPNN, SVM, ELM classifiers. It is observed that the proposed classifier achieved 100% in D-66, 100% in D-160 and 98.95% in D-255 and it is also observed in Figure 8.

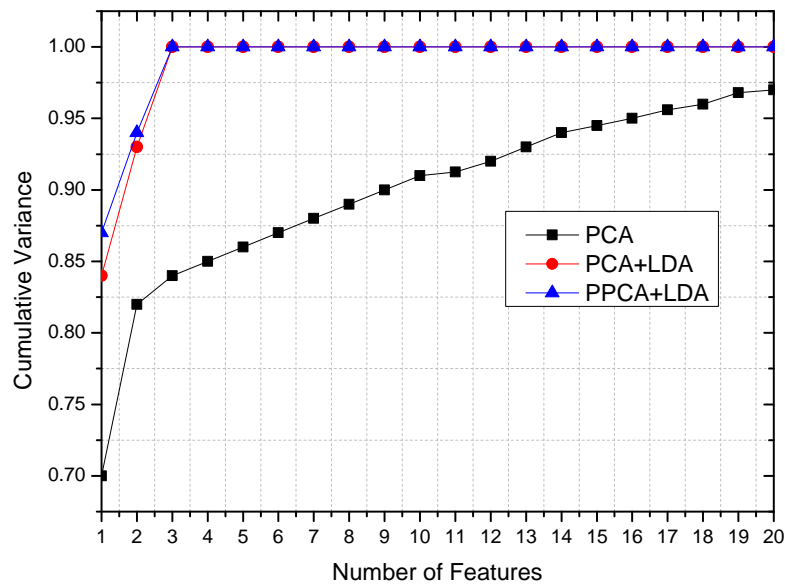


Figure 7: Cumulative Variance Vs number of features for three different datasets

Table 2: Comparison of Classification Accuracy

Classifiers	Accuracy(%)		
	D-66	D-160	D-255
KNN	98.49	98.12	95.69
BPNN	100.00	98.75	95.29
SVM	100.00	100.00	98.82
ELM	100.00	99.94	99.18
FNN-MPSOACO	100.00	100.00	98.95

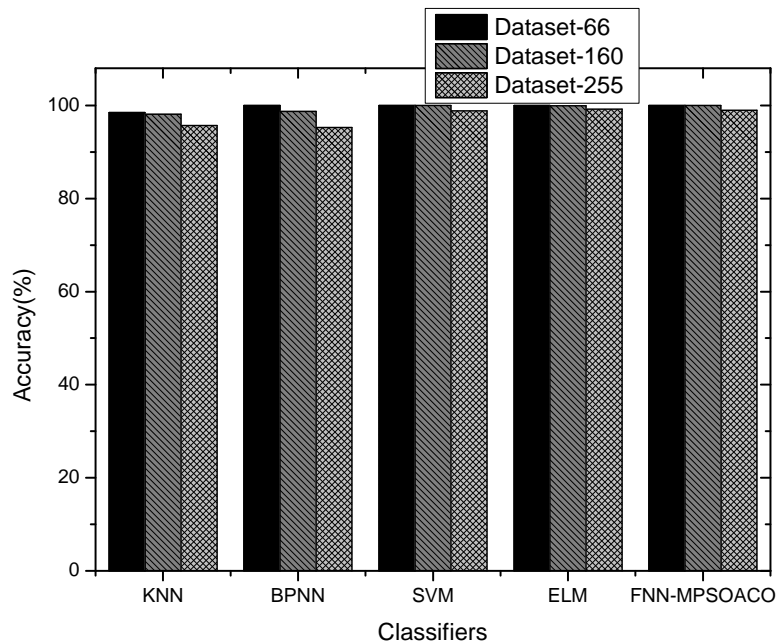


Figure 8: Classification accuracy of KNN, BPNN, SVM, ELM and FNN-MPSOACO over three datasets

The classification accuracy of the proposed method is compared with the existing methods DWT+SVM [35],DWT+SOM [35],DWT+SVM+RBF [35], DWT + PCA + FNN + SCABC [37], DWT + PCA + FNN + ACP SO [38],DWT + PCA + BPNN + SCG [39], DWT + PCA + KSVM [43], DWT + PCA + ADBRF [42], RT + PCA + LS-

SVM [40], WT + PCA + ABC-SPSO-FNN [41], DWT+PCA+k-NN[36], WE + NBC [44] and DWT + SUR + ADBSVM [45] based on the average of the 10 iterations results using the 5-fold cross validation.

To estimate the performance comparison, the size of the population in the algorithms is taken as 100, that consists of 50 particles and 50 ants, a_1 and a_2 values are taken as 2 and ω is taken as 0.75. The maximum iterations are restricted to 1000. Table 3 shows the performance comparison in terms of classification accuracy of the proposed and existing methods. It is observed that the proposed DWT+PPCA+LDA+FNN+MPSOACO achieved 100% in Dataset-66, 100% in Dataset-160 and 99.72% in Dataset 255.

Table 3: Accuracy comparison of different methods

Approaches	Feature	Accuracy (%)		
		D-66	D-160	D-255
DWT+SVM [35]	4761	96.15	95.38	94.05
DWT+SOM[35]	4761	93.99	92.89	91.65
DWT+SVM+RBF [35]	4761	98.00	96.98	96.37
DWT + PCA + FNN + SCABC [37]	19	100.00	98.75	97.38
DWT + PCA + FNN + ACPSO [38]	19	100.00	97.54	96.79
DWT + PCA + BPNN + SCG [39]	19	100.00	98.93	97.81
DWT + PCA + KSVM [43]	19	100.00	98.29	97.14
DWT + PCA + ADBRF [42]	13	100.00	99.30	98.44
RT + PCA + LS-SVM [40]	9	100.00	99.38	98.82
WT + PCA + ABC-SPSO-FNN [41]	7	100.00	98.88	98.43
DWT+PCA+k-NN[36]	7	98.00	97.54	96.79
WE + NBC [44]	7	92.58	99.62	99.02
DWT + SUR + ADBSVM [45]	7	100.00	99.22	98.43
DWT+PPCA+LDA+FNN+MPSOACO (Proposed)	3	100.00	100.00	99.72

4.4 Computing Time Analysis

Table 4 shows the analysis of the computing time for each step in the DWT+PPCA+LDA+FNN+MPSOACO method. The five procedures such as Wiener filter costs 0.252 s, DWT costs 0.685s, PPCA costs 0.243s, LDA costs 0.312s and FNN-MPSOACO costs 202.745s. for online mechanism, Wiener Filter costs 0.002sec, DWT costs 0.003s, PC costs 0.003 sec and prediction will be done in 0.001s.

Table 4: Computing time analysis of the DWT+PPCA+LDA+FNN+MPSOACO for D-255

Offline Learning	Time (s)
Weiner Filter	0.252
DWT	0.685
PPCA	0.243
LDA	0.312
FNN-MPSOACO	202.745
Online Prediction	Time (s)
Weiner Filter	0.002
DWT	0.003
PC	0.003
Prediction	0.001

CONCLUSION

This paper discussed the new model of "DWT+PPCA+LDA+FNN-MPSOACO" for identifying the pathological brains in MR images. The proposed model achieved highest classification accuracy of 99.72%. As an initial step, the proposed method uses Wiener+DWT for extracting the features from images. A PPCA+LDA have been used to perform the normalization and feature reduction. The FNN-MPSOACO algorithm has been used to classify the MR images into normal and pathological brain. The

proposed method achieved highest accuracy with minimum number of features compared to other existing methods. In future, the proposed method is extended with other images like CT scan, PET and MRSI. The proposed method is evaluated over large medical databases by using the deep learning mechanism.

REFERENCES

[1] Mohsin, S. A., N. M. Sheikh, and W. Abbas, "MRI induced heating of artificial bone implants,"

Journal of Electromagnetic Waves and Applications, Vol. 23, No. 5, 799-808, 2009.

- [2] Shafiq, Muhammad Umar, and Ali Iftikhar Butt. "Segmentation of brain MRI using U-Net: Innovations in medical image processing." *Journal of Computational Informatics & Business* 1, no. 1 (2024).
- [3] S. Chaplot, L.M.Patnaik, N.R.Jagannathan, Classification of magnetic resonance brain images using wavelets as input to support vector machine and neural network, *Biomed. Signal Process. Control* 1(1) (2006) 86–92.
- [4] Yadav, Akash, Rakesh Kumar, and Meenu Gupta. "An analysis of convolutional neural network and conventional machine learning for multiclass brain tumor detection." In *AIP Conference Proceedings*, vol. 3072, no. 1. AIP Publishing, 2024.
- [5] E. S. A. El-Dahshan, T. Honsy, A. B. M. Salem, Hybrid intelligent techniques for MRI brain images classification, *Dig. Signal Process.* 20 (2) (2010) 433–441.
- [6] Y. Zhang, S.Wang, L.Wu, A novel method for magnetic resonance brain image classification based on adaptive chaotic PSO, *Prog. Electromagn. Res.* 109 (2010) 325–343.
- [7] El-Dahshan, E. S. A., Hosny, T., & Salem, A. B. M. (2010). Hybrid intelligent techniques for MRI brain images classification. *Digital Signal Processing*, 20(2), 433-441.
- [8] Y. Zhang, S.Wang, L.Wu, A novel method for magnetic resonance brain image classification based on adaptive chaotic PSO, *Prog. Electromagn. Res.* 109 (2010) 325–343.
- [9] Y. Zhang, L.Wu, S.Wang, Magnetic resonance brain image classification by an improved artificial bee colony algorithm, *Prog. Electro magn. Res.* 116 (2011) 65–79.
- [10] Y. Zhang, L.Wu, An MR brain images classifier via principal component analysis and kernel support vector machine, *Prog. Electro magn. Res.* 130 (2012) 369–388.
- [11] Y. Zhang, S.Wang, G.Ji,Z.Dong, An MR brain images classifier system via particle swarm optimization and kernel support vector machine, *Sci. World J.* 2013 (2013)1–9.
- [12] S. Das, M. Chowdhury, M. K. Kundu, Brain MR Image classification using multi scale geometric analysis of ripple, *Prog. Electro magn. Res.* 137 (2013) 1–17.
- [13] M. Saritha, K. P. Joseph, A. T. Mathew, Classification of MRI brain images using combined wavelet entropy based spider webplots and probabilistic neural network, *Pattern Recognit. Lett.* 34 (16) (2013) 2151–2156.
- [14] Khan, Saif Ur Rehman, Ming Zhao, Sohaib Asif, and Xuehan Chen. "Hybrid-NET: A fusion of DenseNet169 and advanced machine learning classifiers for enhanced brain tumor diagnosis." *International Journal of Imaging Systems and Technology* 34, no. 1 (2024): e22975.
- [15] S. Chaplot, L.M. Patnaik, and N. R. Jagannathan, "Classification of magnetic resonance brain images using wavelets as input to support vector machine and neural network," *Biomedical Signal Processing and Control*, vol. 1, no. 1, pp. 86–92, 2006.
- [16] E.S.A. El-Dahshan, T. Honsy , A. B. M. Salem, Hybrid intelligent techniques for MRI brain images classification, *Dig. Signal Process.* 20 (2) (2010) 433 – 441.
- [17] M.E. Tipping, C.M. Bishop, Probabilistic principal component analysis, *J. R. Stat. Soc. Ser. B* 61 (3) (1999) 611–622.
- [18] J. Yang , J.-y. Yang , Why can LDA be performed in PCA transformed space? *Pattern Recognit.* 36 (2) (2003) 563–566 .
- [19] A.M. Martínez , A.C. Kak , PCA versus LDA , *IEEE Trans. Pattern Anal. Mach. Intell.* 23 (2) (2001) 228–233 .
- [20] Y. Zhang, S. Wang, G. Ji, and Z. Dong, An MR brain images classifier system via particle swarm optimization and Kernel support vector machine, *Sci World J* 2013, 2013.
- [21] M. Manoochehri and F. Kolahan, Integration of artificial neural network and simulated annealing algorithm to optimize deep drawing process, *Int J AdvManufTechnol* 73 (2014), 241–249.
- [22] Y. Zhang, S. Balochian, P. Agarwal, V. Bhatnagar, and O.J. Housheya, Artificial intelligence and its applications, *Math ProbEng* 2014 (2014), 10, doi:10.1155/2014/840491.
- [23] Y. Zhang, S. Wang, and Z. Dong, Classification of Alzheimer disease based on structural magnetic resonance imaging by Kernel support vector machine decision tree, *ProgrElectromagn Res* 144 (2014), 171–184.
- [24] Y. Zhang, S. Wang, G. Ji, and P. Phillips, Fruit classification using computer vision and feed forward neural network, *J Food Eng* 143 (2014), 167–177.
- [25] R.C. Eberhart , J. Kennedy , Particle swarm optimization, in: *Proceedings of the IEEE conference on Neural Network*, IEEE, 1995a, pp. 1942–1948 .
- [26] R.C. Eberhart , J. Kennedy , A new optimizer using particle swarm theory, in: *Proceedings of the Sixth International Symposium on Micro Machine and Human Science*, IEEE, 1995b, pp. 39–43 .
- [27] Coloni, A., et al. 1992. Distributed optimization by ant colonies. In *Toward a Practice of Autonomous Systems: Proceedings of the First European Conference on Artificial Life* (eds. Verela, F.J. and Bourguine, P.), pp. 134-142. MIT Press, Cambridge, USA.
- [28] Caro, G.D. and Dorigo, M. 1998. AntNet: distributed stigmergetic control for communications networks. *J. Artif. Intell. Res.* 9: 317-365.
- [29] Parpinelli, R.S., et al. 2002. Data mining with an ant colony optimization algorithm. *IEEE Trans. Evol. Comput.* 6: 321-332.
- [30] Shmygelska, A. and Hoos, H.H. 2005. An ant colony optimization algorithm for the 2D and 3D

hydrophobic polar protein folding problem. *BMC Bioinformatics* 6:30.

[31] <http://med.harvard.edu/AANLIB/> accessed on 12/06/2019

[32] Soomro, Toufique A., Lihong Zheng, Ahmed J. Afifi, Ahmed Ali, Shafiullah Soomro, Ming Yin, and Junbin Gao. "Image segmentation for MR brain tumor detection using machine learning: a review." *IEEE Reviews in Biomedical Engineering* 16 (2022): 70-90.

[33] Brindha, P. Gokila, M. Kavinraj, P. Manivasakam, and P. Prasanth. "Brain tumor detection from MRI images using deep learning techniques." In *IOP conference series: materials science and engineering*, vol. 1055, no. 1, p. 012115. IOP Publishing, 2021.

[34] Y. Zhang , Y. Sun , P. Phillips , G. Liu , X. Zhou , S. Wang ,A multilayer perceptron based smart pathological brain detection system by fractional Fourier entropy, *J. Med. Syst.* 40 (7) (2016) 1–11 .

[35] Khan, Md Saikat Islam, Anichur Rahman, Tanoy Debnath, Md Razaul Karim, Mostofa Kamal Nasir, Shahab S. Band, Amir Mosavi, and Iman Dehzangi. "Accurate brain tumor detection using deep convolutional neural network." *Computational and Structural Biotechnology Journal* 20 (2022): 4733-4745.

[36] Arabahmadi, Mahsa, Reza Farahbakhsh, and Javad Rezazadeh. "Deep learning for smart Healthcare—A survey on brain tumor detection from medical imaging." *Sensors* 22, no. 5 (2022): 1960.

[37] Y. Zhang, L.Wu, and S.Wang, "Magnetic resonance brain image classification by an improved artificial bee colony algorithm," *Progress In Electromagnetics Research*, vol. 130, pp. 369–388, 2012.

[38] Y. Zhang, S. Wang, and L. Wu, "A novel method for magnetic resonance brain image classification based on adaptive chaotic PSO," *Progress in Electromagnetics Research*, vol. 109, pp. 325–343, 2010.

[39] G.Viswanath & Dr.G.Swapna "Health Prediction Using Machine Learning with Drive HQ Cloud Security" in *Frontiersin Health Informatics*, 2024. Vol. 13, No. 8, pp. 2755-2761.

[40] S. Das, M. Chowdhury, and M. K. Kundu, "Brain MR image classification using multi-scale geometric analysis of ripplelet," *Progress in Electromagnetics Research*, vol. 137, pp. 1–17, 2013.

[41] S. Wang, Y. Zhang, Z. Dong et al., "Feed-forward neural network optimized by hybridization of PSO and ABC for abnormal brain detection," *International Journal of Imaging Systems and Technology*, vol. 25, no. 2, pp. 153–164, 2015.

[42] D. R. Nayak, R. Dash, and B. Majhi, "Brain MR image classification using two-dimensional discrete wavelet transform and AdaBoost with random forests," *Neurocomputing*, vol. 177, pp.188–197, 2016.

[43] Zhang and L. Wu, "An MR brain images classifier via principal component analysis and kernel support vector machine," *Progress in Electromagnetics Research*, vol. 130, pp. 369–388, 2012.

[44] S. Roweis, "EM algorithms for PCA and SPCA," in *Advance in Neural Information Processing System*, vol. 10, pp. 626–632, MIT Press, Cambridge, MA, USA, 1998.

[45] D. R. Nayak, R. Dash, and B. Majhi, "Stationary wavelet transform and AdaBoost with SVM based pathological brain detection in MRI scanning," *CNS and Neurological Disorders -Drug Targets*, vol. 16, no. 2, pp. 137–149, 2017.

[46] Mudukshiwale, Amit D., and Y. M. Patil. "Brain Tumor Detection Using Digital Image Processing." *Brain* 6, no. 05 (2019).

[47] G.Viswanath & G.Swapna, "Data Mining-Driven Multi-Feature Selection for Chronic Disease Forecasting", in *Journal of Neonatal Surgery*,2025, Vol.14, No. 5s, pp. 108-124.

[48] Sharma, Manorama, G. N. Purohit, and Saurabh Mukherjee. "Information retrieves from brain MRI images for tumor detection using hybrid technique K-means and artificial neural network (KMANN)." In *Networking communication and data knowledge engineering*, pp. 145-157. Springer, Singapore, 2018.

[49] Nagalkar, Vinay J., and G. G. Sarate. "Brain Tumor Detection and Identification using Support Vector Machine." *Brain* 6, no. 12 (2019).

[50] Padlia, Minal, and Jankiballabh Sharma. "Fractional Sobel filter based brain tumor detection and segmentation using statistical features and SVM." In *Nanoelectronics, circuits and communication systems*, pp. 161-175. Springer, Singapore, 2019.